Int. J. Morphol.,
43(6):1973-1980, 2025.

Histology and Immunofluorescence Analyses in the Brain of Reeves' Turtle (*Mauremys reevesii*)

Histología y Análisis de Inmunofluorescencia en el Cerebro de la Tortuga de Reeve (*Mauremys reevesii*)

Ruiyun Liu[1]; Peng Liu[1]; Hong Chen[2]; Yu Wang[1]; Zimo Li[3]; Zaiqun Liu[1] & Liuwang Nie[1]

LIU, R; LIU, P.; CHEN, H.; WANG, Y.; LI, Z.; LIU, Z. & NIE, L. Histology and immunofluorescence analyses in the brain of Reeves' turtle (*Mauremys reevesii*). *Int. J. Morphol., 43(6)*:1973-1980, 2025.

SUMMARY: This study investigated the histological structure of the *Mauremys reevesii* brain using hematoxylin-eosin (HE) staining and examined the localization and expression of Pax6 in the brain through immunofluorescence staining. The HE staining results revealed the histological structures in the olfactory bulb, cerebrum, diencephalon, mesencephalon, cerebellum and medulla oblongata of *M. reevesii*. The olfactory bulb could be divided into seven layers from the outer to the inner region. The cerebral cortex consisted of three layers. The optic tectum of mesencephalon comprised six distinct layers. The cerebellar cortex exhibited a three-layered organization. In *M. reevesii*, while the thalamus and medulla oblongata lacked distinct laminar organization, they contained numerous nuclei. Immunofluorescence staining revealed widespread distribution of Pax6-immunoreactive (Pax6-IR) cells in the brain of *M. reevesii*. In the olfactory bulb, Pax6-IR cells were densely distributed in the glomerular layer. Within the telencephalon, these cells showed the highest density and strongest fluorescence intensity in the dorsal septum. In the diencephalon of *M. reevesii*, the prethalamus contained extensive Pax6-IR cell populations. Within the mesencephalon, prominent Pax6 immunoreactivity was observed in the tegmentum. In coronal sections, continuous Pax6-IR cells were prominently distributed along the dorsal medulla oblongata near the alar plate region of the fourth ventricle. In the cerebellum, extensive Pax6 immunoreactivity was observed in both the medullary layer and granular layer, albeit with weaker fluorescence intensity.

KEY WORDS: ***Mauremys reevesii*** **Brain; HE staining; Pax6; Immunofluorescence staining.**

INTRODUCTION

The Reeves' turtle (*Mauremys reevesii*), a chelonian species of order Testudines, was currently listed as Endangered (EN) due to population declines caused by habitat degradation and overharvesting. This commercially significant aquaculture species was designated as a Class II Protected Animal in China. Current research on turtle brain included studies of specific brain structures and functions. Liu & Li (2005), examined the pituitary gland in *M. reevesii* and identified 5 secretory hormone cell types. Shen *et al.* (1994), analyzed synaptic structures in the telencephalic anterior dorsal ventricular ridge of *M. reevesii*. Other studies had investigated the distribution of neurotransmitters and functional proteins in the turtle nervous system, including neuropeptides (NFPP) (Muñoz *et al*., 2008), transferrin-binding protein (TfBP) (Park *et al*., 2009), and glial fibrillary acidic protein (GFAP) (Kálmán *et al*., 1994) in the brain of *Pseudemys scripta elegans*. Additionally, Jiménez *et al*. (2024), created the MRI-based atlas of the forebrain in *Trachemys scripta*.

Pax6, a crucial transcription factor in the Pax gene family, plays pivotal roles in neural development (More *et al*., 2024). Pax6 not only regulates the proliferation and differentiation of neural stem cells, influencing their fate, but also interacts with proteins such as Wnt3a to modulate cortical neurogenesis as well as neuronal proliferation and migration (Zhang *et al*., 2025). Additionally, it plays a role in establishing boundaries between regions of the vertebrate central nervous system (Kozmik & Kozmikova, 2024). As a crucial neural transcription factor, Pax6's distribution had been characterized in teleosts (López *et al*., 2020), amphibians (Bandín *et al*., 2014), birds (Nomura *et al*., 1998),

[1] College of Life Sciences, Anhui Normal University, Wuhu, Anhui, China.
[2] Anhui Normal University Library, Wuhu, Anhui, China.
[3] Trinity College, The University of Melbourne, Melbourne, Australia.
FUNDING. This study was funded by Anhui Provincial Key Laboratory of the Conservation and Exploitation of Biological Resources, the Anhui Provincial Key Laboratory of Molecular Enzymology and Mechanism of Major Diseases (No. KJ2020A0083).

Received: 2025-07-18 Accepted: 2025-09-08

and mammals (Daems *et al*., 2025), but remained poorly studied in reptilian brains. This study therefore focused on mapping Pax6 expression in the brain of *M. reevesii.*

Given the limited research on whole-brain organization in *M. reevesii*, this study systematically characterized the histological architecture of the *M. reevesii* brain using HE staining and localized Pax6-IR cells through immunofluorescence staining.

MATERIAL AND METHOD

Experimental Materials. Two adult *M. reevesii* (3 years old) with a body length of about 15 cm and two juvenile *M. reevesii* (5 months old) with a body length of about 5 cm were purchased from Zhejiang Tortoise Breeding Park (Fig. 1 A, D). After ether anesthesia, the whole brain tissue was rapidly stripped from the cranial cavity, and the brain length of adult turtles was about 2 cm (Fig. 1 B, C), and that of juvenile turtles was about 1.2 cm (Fig. 1 E, F). The above procedures were approved by the Chinese Forestry Department and the Animal Ethics Committee of Anhui Normal University (Certificate No. 2018012). Brain tissues were fixed with paraformaldehyde for 24 h, then routinely dehydrated, transparent, paraffin-embedded, and serially sliced on a Leica slicer (about 8 μm thick), and dried in an oven at 37 °C after retrieval of the slices. The paraffin sections of adult *M. reevesii* brains were selected for HE staining to observe the histological structure of the brain, while the paraffin sections of juvenile *M. reevesii* brains were used for immunofluorescence staining.

HE Staining. After drying, one section was selected every 10 spacing, and the section was put into xylene for dewaxing and then rehydrated by gradient alcohol and distilled water, and the processed sections were stained by hematoxylin for 3 min, rinsed in tap water and then differentiated by differentiation solution for 2-5 s, rinsed in tapwater and then returned to blue by return blue solution for 2-5 s, and stained in eosin stain for 5 min after rinsing in tap water, and finally, dehydrated by gradient alcohol and clarified in xylene and then sealed the film with Neutral gum. After staining, the slices were observed and photographed with a Leica Mateo FL digital inverted microscope.

Immunofluorescence Staining. Paraffin sections were dewaxed and rehydrated; treated sections were placed in a microwave oven for thermal repair of antigens; 0.1% TritonX-100 was permeabilized for 10 min; 3 % BSA blocking solution was added dropwise and blocked for 50 min at room temperature; appropriately diluted primary antibody (PAX6 Rabbit mAb, A24118, Abletec Biologicals) was added dropwise, and the cells were incubated at room temperature for 1 h at 37 °C with fluorescent secondary antibody (Alexa Flour 488 labelled goat anti-rabbit IgG, GB25303, Servicebio) for 1 h, then the nuclei of the cells were re-stained with DAPI to avoid the light; finally, anti-fluorescent bursting agent was added dropwise on the tissues to seal the film. After the end of staining, it could be observed and photographed with a Leica Mateo FL digital inverted microscope.

Table I summarizes the abbreviations used throughout the manuscript. Anatomical structures are listed in alphabetical order, followed by their corresponding abbreviations, to facilitate reading and comprehension of the text.

RESULTS

The histological structure of brain in *M. reevesii* by HE staining

The *M. reevesii* brain consisted of the olfactory bulb, cerebrum, diencephalon, mesencephalon, cerebellum and medulla oblongata from rostral to caudal side (Fig. 2A), while

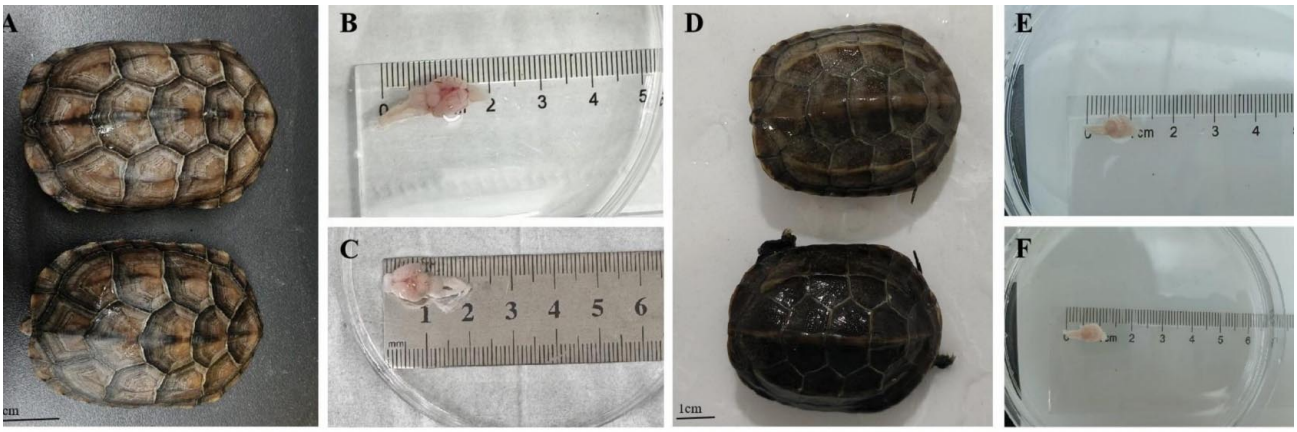

Fig.1. *M. reevesii* and brain specimen. (A) Adult *M. reevesii*. Scale bar: 5 cm; (B-C) Brain tissue of adult *M. reevesii*; (D) Juvenile *M. reevesii*. Scale bar: 1 cm; (E-F) Brain tissue of juvenile *M. reevesii*.

Table I. Abbreviations.The structures were listed alphabetically, followed by their abbreviations.

Acc	nucleus accumbens	OPL	outer plexiform layer
Alar	Alar plate	OT	optic tectum
Basal	Basal plate	OV	olfactory ventricle
CAq	cerebral aqueduct	p1-p3	prosomeres 1-3
CB	cerebellum	Pa	pallium
CbC	cerebellar cortex	PC	Purkinje cells
CbM	cerebellar medulla	Pc	posterior commissure
CeA	central amygdala	Pe	posterior olfactory eminence
CL	cellular layer	PH	periventricularis hypothalami
CPI	choroid plexus	PL	Purkinje layer
CV	cerebellar ventricle	PT	pretectum
DB	diagonal band	PTh	prethalamus
DCN	Cerebellar Deep Nuclei	PThE	prethalamic eminence
DCx	dorsal cortex	PVO	paraventricular organ
Dm	nucleus dorsomedialis thalami	Pyr	Pyramidal cells
DMCx	dorsomedial cortex	Ra	raphe nucleus
dStr	dorsal striatum	RF	reticular formation
DVR	dorsal ventricular ridge	Ri	inferior reticular nucleus
ECL	ependymal cell layer	Rs	superior reticular nucleus
EPL	external plexiform layer	Rt	nucleus rotundus thalami
GL	glomerular layer	SAC	stratum album centrale
GrL	granule cell layer	Sd	septum dorsalis
Hb	habenula nucleus	SFGS	stratum fibrosum et griseum superficiale
HY	hypothalamus	SFP	stratum fibrosum periventriculare
IPL	internal plexiform layer	SGC	stratum griseum centrale
LCx	lateral cortex	SGP	stratum griseum periventriculare
LV	lateral ventricle	SnV	sensory nucleus of trigeminal nerve
MCL	mitral cell layer	SO	stratum opticum
MCx	medial cortex	SPV	supraoptic paraventricular nucleus
MeA	medial amygdala	Str	striatum
Mes	mesencephalon	tc	tectal commissure
ML	molecular layer	Tel	telencephalon
mlf	medial longitudinal fasciculus	Tgd	dorsal tegmentum
MnV	motor nucleus of trigeminal nerve	TH	thalamus
MO	medulla oblongata	Tub	tuberal area of the hypothalamus
Mt	medial thalamic nucleus	V	ventricle
OB	olfactory bulb	Ve	vestibular nucleus
oc	optic chiasm	VO	ventricle optic
ONL	olfactory nerve layer		

cerebrum included the dorsal ventricular ridge (DVR), striatum (Str), medial amygdala (MeA), and the lateral ventricles (LV) inside. The diencephalon of *M. reevesii* comprised three prosomeres (p1-p3) (p1 contained the pretectal area, p2 included most thalamus, and p3 encompassed the prethalamic region). The mesencephalon primarily contained the optic tectum (OT) and tegmentum (teg).

The olfactory bulb served as a crucial relay station for transmitting olfactory signals from the olfactory epithelium to higher centers, positioned at the rostral extremity of the brain and connecting with the cerebrum (Fig. 2A). Its internal cavity, the olfactory ventricle (OV), communicated with the cerebral lateral ventricles (Fig. 2 A, B). In *M. reevesii*, the laminar organization of the olfactory bulb resembled the mammalian surface-to-core stratification pattern, exhibiting distinct layers. Both coronal and sagittal sections revealed the following sequential layers from exterior to interior: the olfactory nerve layer (ONL), glomerular layer (GL), external plexiform layer (EPL), mitral cell layer (MCL), internal plexiform layer (IPL), and granule cell layer (GrL). Adjacent to the olfactory ventricle laid an additional ependymal cell layer (ECL). Notably, the granule cell layer demonstrated significantly greater thickness compared to other layers (Fig. 2 C, D).

The cerebrum of *M. reevesii* connected with the olfactory bulb (Fig. 2A). As the central component of the forebrain, it displayed primitive yet functionally differentiated architecture, consisting of dorsal cortical areas and basal nuclear regions. Bordered by the longitudinal cerebral fissure, the brain was divided into bilateral hemispheres, each containing a C-shaped lateral ventricle (Fig. 2E). In coronal sections of the cerebral hemispheres, the following structures were observed sequentially from dorsal to ventral: the cerebral cortex, dorsal ventricular ridge (DVR), striatum (Str), nucleus accumbens (Acc), diagonal band (DB), and the septum dorsalis (Sd) where the medial aspects of both hemispheres approximate each other (Fig. 2E). The cerebral cortex could be subdivided into four distinct regions based on anatomical position: the medial cortex (MCx), dorsomedial cortex (DMCx), dorsal cortex (DCx), and lateral cortex (LCx) (Fig. 2E). The cerebral cortex was composed of three layers from the superficial to the deep layer, sequentially as follows: the outer plexiform layer (OPL), the cellular layer (CL), and the inner plexiform layer (IPL) (Fig. 2F). The cellular layer (CL) demonstrated the highest neuronal density, containing characteristic pyramidal neurons (Pyr) commonly observed in cerebral cortices (Fig. 2G).

The diencephalon connected with the telencephalon and was situated between the cerebral hemispheres, primarily comprising the thalamus and hypothalamus (Fig. 2A). In coronal sections, the third ventricle (3V) divided the thalamus into bilaterally symmetrical parts (Fig. 2H). The most prominent thalamic nucleus was the nucleus rotundus (Rt), exhibiting a circular morphology (Fig. 2I). Ventral to the nucleus rotundus (Rt) and dorsal to the third ventricle (3V) laid the medial thalamic nucleus (Mt) (Fig. 2I). The habenular nucleus (Hb) was located at the dorsomedial angle of the dorsal thalamus, presenting as paired structures (Fig. 2I). The hypothalamic region laid ventral to the thalamus, with the hypothalamus (HY) constituting the largest diencephalic component. This region contained the supraoptic paraventricular nucleus (SPV), with the tuberal region (Tub) situated caudally, housing the ventromedial hypothalamus (Vmh). The optic chiasm (OC) was visible at the basal hypothalamus (Fig. 2H). Furthermore, in the coronal sections of the thalamus in *M. reevesii*, prosomere 1(p1), prosomere 2(p2) and prosomere 3(p3) could be seen in order from top to bottom (Fig. 2H).

The mesencephalon (also named the optic lobe) connected with the diencephalon dorsally and consisted of three primary components: the optic tectum (OT), tegmentum (Teg), and cerebral aqueduct (Fig. 2A). The optic

tectum occupied the most dorsal position within the mesencephalon and contained an internal cavity termed the ventricle optic (VO) (Fig. 2J). Coronal sections demonstrated that the tectal commissure (TC) bridged the bilateral optic tecta, with the posterior commissure (PC) located ventrally (Fig. 2J). The degree of laminar organization generally reflected the sophistication of visual processing, with *M. reevesii* optic tectum displaying six distinct layers from superficial to deep: the stratum opticum (SO), stratum fibrosum et griseum superficiale (SFGS), stratum griseum centrale (SGC), stratum album centrale (SAC), stratum griseumperiventriculare (SGP), and stratum fibrosum periventriculare (SFP). The medial cavity of the mesencephalon was the ventricle optic (VO), and a layer of ependymal cells (ECL) covered the outer surface of the ventricle optic (Fig. 2 K, L). The tegmentum (Teg) was located on the ventral side of the mesencephalon, and the cerebral aqueduct (CAq) connected the ventricle optic (VO) with the third ventricle (3V) (Fig. 2J).

The medulla oblongata was located at the caudal end of the brain and, together with the mesencephalon, formed the brainstem. The cavity formed dorsally by the medulla and cerebellum was called the fourth ventricle (4V) (Fig. 2 A, M). Near the midline on the dorsal side of the medulla, the medial longitudinal fasciculus could be observed, closely adjacent to the floor of the fourth ventricle (4V) and medially neighboring the raphe nucleus (Ra). In cross-section, the medial longitudinal fasciculus (mlf) appeared as a symmetrical bilateral band-like structure with dense fibers (Fig. 2N). The raphe nucleus (Ra) contained numerous neurons with spindle-shaped or oval cell bodies, and their dendrites extended bilaterally along the midline

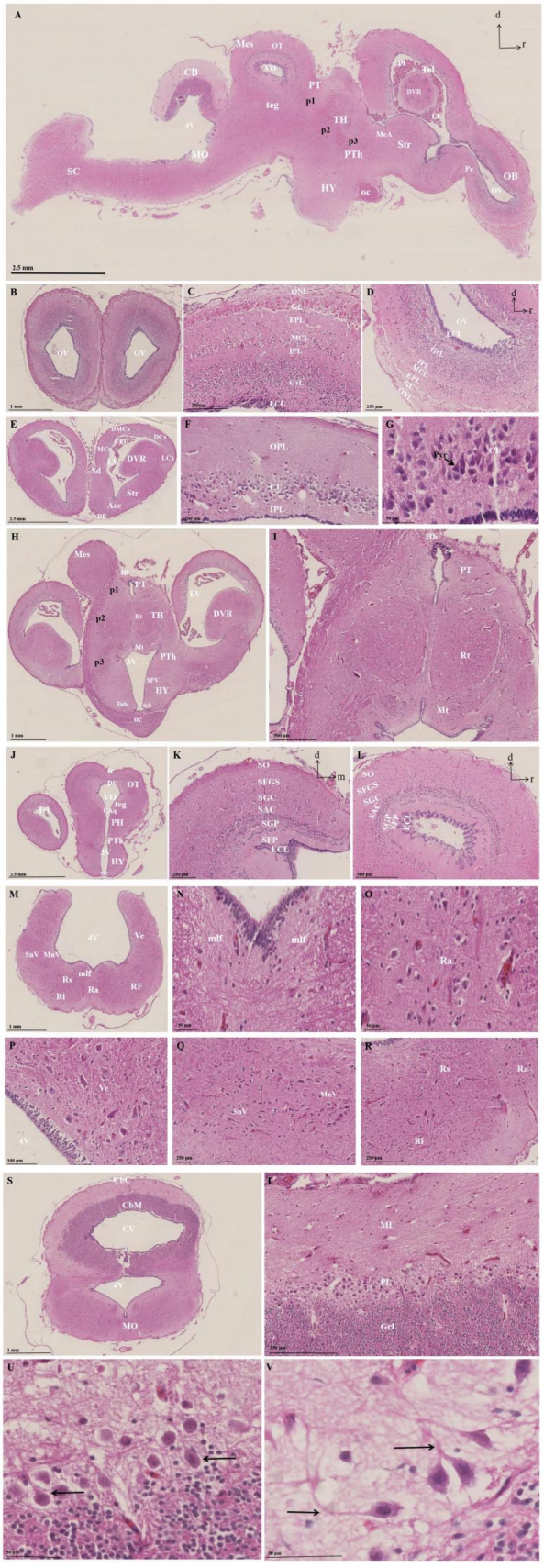

Fig. 2. Histological slices through the adult *M. reevesii* brain (HE staining). (A) Sagittal section of *M. reevesii* whole brain. Scale bar: 2.5 mm; (B) The olfactory bulb (OB) in coronal section. Scale bar: 1 mm; (C) Layered structure in coronal section. Scale bar: 250 μm; (D) Layered structure in sagittal section. Scale bar: 250 μm; (E) The cerebrum in coronal section. Scale bar: 2.5 mm; (F) Layers of the cerebral cortex. Scale bar: 100 μm; (G) The pyramidal cell (Pyr) in the cell layer. Scale bar: 50 μm; (H) The diencephalon in coronal section. Scale bar: 1 mm; (I) nucleus rotundus thalami (Rt) and medial thalamic nucleus (Mt). Scale bar: 500 μm; (J) The mesencephalon in coronal section. Scale bar: 2.5 mm; (K) Layers of the the optic tectum (OT) in coronal section. Scale bar: 250 μm; (L) Layers of the optic tectum (OT) in sagittal section. Scale bar: 500 μm; (M) The medulla oblongata in coronal section. Scale bar: 1 mm; (N) Medial longitudinal fasciculus (mlf). Scale bar: 50 μm; (O) raphe nucleus (Ra). Scale bar: 50 μm; (P) vestibular nucleus (Ve). Scale bar: 100 μm; (Q) motor nucleus of trigeminal nerve (MnV) and sensory nucleus of trigeminal nerve (SnV). Scale bar: 250 μm; (R) superior reticular nucleus (Rs) and inferior reticular nucleus (Ri). Scale bar: 250 μm; (S) The cerebellum and medulla oblongata (MO) in coronal section. Scale bar: 1 mm; (T) Layers of the cerebellar cortex. Scale bar: 250 μm; (U) Purkinje cells. Scale bar: 50 μm; (V) The dendrite of Purkinje cell. Scale bar: 50 μm. (d: dorsal; r: rostral; m: medial; ←: showing the Purkinje cell; →: showing the dendrite of Purkinje cell).

(Fig. 2O). Additionally, on the coronal sections, various nuclear structures such as the vestibular nucleus (Ve) (Fig. 2P), the sensory nucleus of the trigeminal nerve (SnV), the motor nucleus of the trigeminal nerve (MnV) (Fig. 2Q), the superior reticular nucleus (Rs), and the inferior reticular nucleus (Ri) (Fig. 2R) could be observed.

The cerebellum of *M. reevesii* was located posterior to the optic tectum (OT) and consisted of two parts: the cerebellar medulla and cerebellar cortex (Fig. 2 A, S). In the coronal section of the cerebellum, a nearly circular cavity was present within the medulla, known as the cerebellar ventricle (CV). The cerebellum and the underlying brainstem enclosed the fourth ventricle (4V) (Fig. 2S). The cerebellar cortex of *M. reevesii* exhibited a typical three-layered structure, consisting of the molecular layer (ML), Purkinje cell layer (PL), and granular layer (GrL) from the outer to the inner region (Fig. 2T). The figure showed that the cerebellar Purkinje cells in *M. reevesii* were arranged in multiple layers, with large pear-shaped soma (Fig. 2U). Thick primary dendrites emerged from the apical portion of the somata and extended vertically upward into the molecular layer (Fig. 2V).

Pax6 localization and expression in the brain of *M. reevesii* by IF staining

Pax6 showed moderate expression in the olfactory bulb of the *M. reevesii*. On sagittal sections, Pax6-IR cells extended from the rostral to caudal side of the olfactory bulb reaching the rostral end of the telencephalon, forming a prominent cluster of Pax6-IR cells in the posterior olfactory eminence (Pe) (Fig. 3A, B). Additionally, the expression was

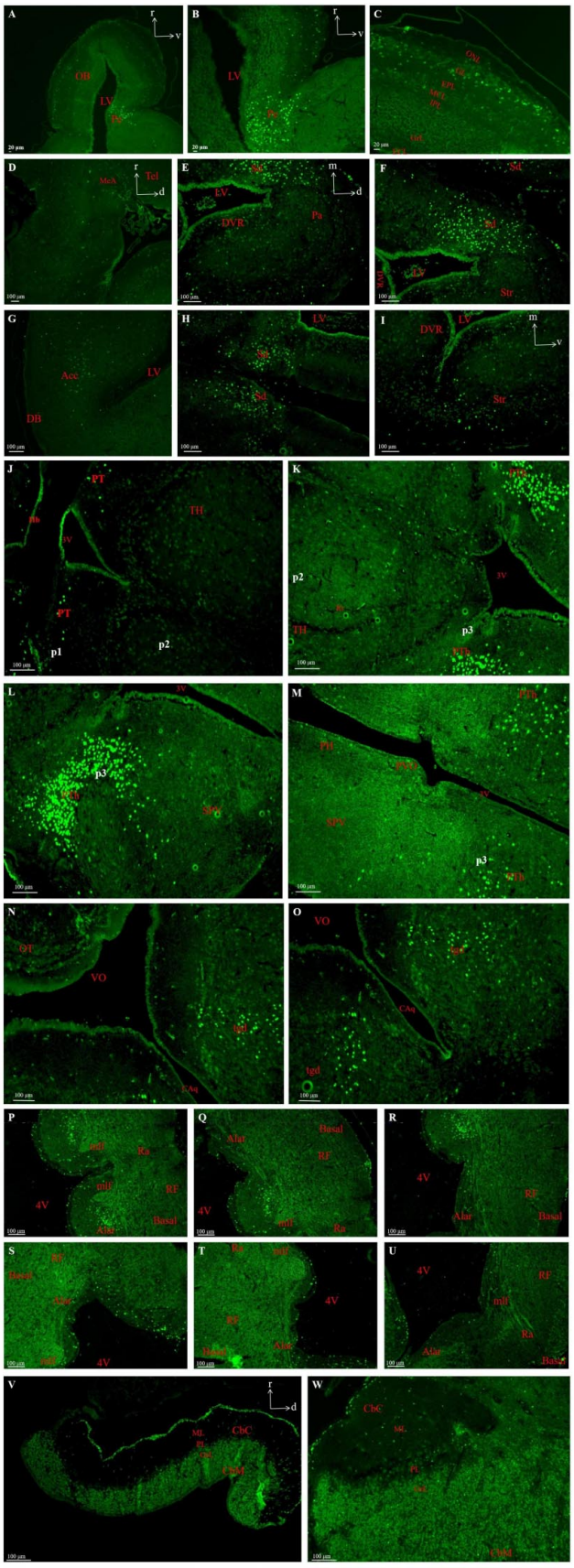

Fig. 3. Immunofluorescent slices through the juvenile *M. reevesii* brain (IF staining). (A)Pax6-IR cells in the olfactory bulb(OB) in the sagittal section. Scale bar: 20 μm; (B) Pax6-IR cells in the posterior olfactory eminence (Pe). Scale bar: 20 μm; (C) Pax6-IR cells in the glomerular layer (GL) of the olfactory bulb (OB). Scale bar: 20 μm; (D) Pax6-IR cells in the medial amygdala (MeA). Scale bar: 100 μm; (E)Pax6-IR cells in the pallium (Pa), septum dorsalis (Sd) and dorsal ventricular ridge (DVR) regions. Scale bar: 100 μm; (F) Pax6-IR cells in the septum dorsalis (Sd) and striatum (Str) regions. Scale bar: 100 μm; (G) Pax6-IR cells in the nucleus accumbens (Acc). Scale bar: 100 μm; (H) Pax6-IR cells in the septum dorsalis (Sd) region of both cerebral hemispheres. Scale bar: 100 μm; (I) Pax6-IR cells in the striatum (Str) region. Scale bar: 100 μm; (J) Pax6-IR cells in pretectum (PT) region. Scale bar: 100 μm; (K-M) Pax6-IR cells in prethalamus (PTh) region. Scale bar: 100 μm; (N-O) Pax6-IR cells in the tegmentum region. Scale bar: 100 μm; (P-U) Pax6-IR cells in the alar plate (dorsal region) of medulla oblongata in the coronal sections. Scale bar: 100 μm; (V) Distribution of Pax6-IR cells in the sagittal section of the cerebellum. Scale bar: 100 μm; (W) Pax6-IR cells in the coronal section of the cerebellum. Scale bar: 100 μm. (r: rostral; v: ventral; d: dorsal; m: medial).

predominantly localized in the peripheral region of the olfactory bulb, with particularly dense distribution of Pax6-IR cells in the glomerular layer (GL) among the multiple layers of the olfactory bulb (Fig. 3C).

Sagittal section analysis (Fig. 3D) revealed Pax6-IR cell expression localized to the medial amygdala (MeA) structure in the ventromedial region of the cerebral hemisphere adjacent to the diencephalon. Coronal section analysis (Fig. 3 E, F, G,H, I) further demonstrated a widespread distribution pattern of Pax6-IR cells throughout the brain, with expression regions including but not limited to: the pallium, dorsal ventricular ridge, septum dorsalis, striatum, and nucleus accumbens among other key nuclei. Notably, the septal region exhibited a significant enrichment of Pax6-IR cells, with cell density markedly higher than other observed regions.

The diencephalon of *M. reevesii* primarily consisted of the thalamus and hypothalamus, which as previously described could be divided into three segments: prosomeres 1-3 (p1-p3). Coronal sections of the *M. reevesii*'s diencephalon revealed that Pax6-IR cells were distributed from dorsal to ventral in both the pretectum and prethalamus, corresponding to the p1 and p3 regions (Fig. 3 J, K, L, M). Notably, the prethalamus exhibited particularly prominent Pax6 positivity, displaying an inverted C-shaped cluster of positive cells (Fig. 3L).

The brainstem of *M. reevesii*, comprising the mesencephalon and medulla oblongata, also exhibited Pax6-IR distribution. In the mesencephalon region, distinct Pax6-IR expression was observed in the dorsal tegmentum (tgd). Coronal sections revealed bilaterally symmetric distribution of positive cells in the tegmental areas flanking the mesencephalic aqueduct (Fig. 3 N, O). Notably, other mesencephalon regions such as the tectal area showed no Pax6-IR cell distribution.

In the coronal sections of the medulla-cerebellum junction, dense clusters of Pax6-IR cells were observed near the medial longitudinal fasciculus (Fig.3 P, Q). Additionally, a prominent continuous distribution of Pax6-IR cells was found in the alar region of the entire medulla, close to the fourth ventricle, with positive cells extending throughout the dorsal aspect of the coronal sections (Fig.3 R, S, T, U).

In the cerebellar region of *M. reevesii*, a distinct Pax6-IR distribution was still present. As previously mentioned, the cerebellum of *M. reevesii* consisted of the cortex and medulla. The cerebellar cortex could be divided into three layers from outer to inner: the molecular layer, Purkinje cell layer, and granular cell layer (Fig. 3V). Sagittal and coronal sections of the *M. reevesii*'s cerebellum revealed a small number of Pax6-IR cells in the molecular layer of the cerebellar cortex, while Purkinje cells showed no Pax6 positivity. The boundary between the cerebellar medulla and granular cell layer was indistinct, exhibiting extensive Pax6-IR staining (Fig.3 V, W).

DISCUSSION

The histological structure compared with other reptile brain

The laminar pattern of the olfactory bulb in reptiles was closer to the surface-to-center layering observed in mammals, exhibiting distinct stratified structures. However, variations existed among different reptiles. For instance, the olfactory bulb of the *Elaphe quadrivirgata* could be divided into six layers from outer to inner: the olfactory nerve fiber layer, glomerular layer, mitral cell layer, inner plexiform layer, granule cell layer, and ependymal cell layer, with the granule cell layer being thinner than the inner plexiform layer (Kondoh *et al*., 2013). Studies on *Pseudemys scripta elegans* revealed a laminar pattern consisting of six layers: the glomerular layer, outer plexiform layer, mitral cell layer, inner plexiform layer, granule cell layer, and internal ependymal cell layer (Smeets *et al*., 2003). Another study on *Scincella tsinlingensis* demonstrated that its olfactory bulb comprised seven layers, from outer to inner: the olfactory nerve layer, glomerular layer, external plexiform layer, mitral cell layer, internal plexiform layer, granular cell layer, and ependymal cell layer, with the granular cell layer being substantially thicker than the internal plexiform layer (Yang *et al*., 2020). In this study, the laminar pattern of the *M. reevesii*'s olfactory bulb was consistent with that of the *Scincella tsinlingensis*. We speculated that these layer differences among reptiles' olfactory bulb may correlate with varying locomotor patterns and ecological behavioral demands.

The laminar organization of the cerebral cortex varied among reptiles. Some reptilian species exhibited a four-layered cortex, such as the Chinese alligator (*Alligator sinensis*), where the cortex consisted of the molecular layer (ML), superficial plexiform layer (SPL), cellular layer (CL), and deep plexiform layer (DPL) from outer to inner (Sarkar & Atoji, 2018). However, most reptiles displayed a three-layered cortex, including *Scincella tsinlingensis* (Yang *et al*., 2020), *Pseudemys scripta elegans* (Sarkar & Atoji, 2018), and *Podarcis hispanica* (Martínez-Guijarro *et al*., 1994). This study revealed that the cerebral cortex of *M. reevesii* consisted of three layers from outer to inner: the outer plexiform layer (OPL), cellular layer (CL), and inner plexiform layer (IPL), consistent with the three-layered pattern observed in most reptilian species.

The layers of the optic tectum in reptiles showed no consistent pattern across species. Studies indicated the optic tectum of *Iguana iguana* could be subdivided into 14 layers (Foster & Hall, 1975). *Clemmys japonica* exhibited 11 tectal layers (Ueda *et al*., 1983), and *Thamnophis sirtalis* showed 7 layers (Dacey & Ulinski, 1986). Research on *Pseudemys scripta elegans* had revealed that its optic tectum could be divided into six layers, from outer to inner: the stratum opticum (SO), stratum fibrosum et griseum superficiale (SFGS), stratum griseum centrale (SGC), stratum album centrale (SAC), stratum griseum periventriculare (SGP), and stratum fibrosum periventriculare (SFP) (Schechter & Ulinski, 1979). In this study, the layer pattern of *M. reevesii*'s optic tectum was largely consistent with *Pseudemys scripta elegans*. We speculated these variations may result from distinct visual requirements among species.

The Pax6 distribution patterns compared with other reptile brain

Currently, substantial research data had been accumulated regarding the distribution patterns of Pax6 in vertebrate brains, but studies focusing on reptiles remained relatively limited. Only a few relevant studies existed, such as investigations of Pax6-IR distribution in the diencephalon and mesencephalon of *Alligator mississipiensis* and comparative studies of Pax6 distribution patterns between *Pseudemys scripta* and other vertebrates. Research showed that Pax6 was strongly expressed in prosomere 1 (p1) and prosomere 3 (p3) of the alligator diencephalon, as well as in the tegmental region of the mesencephalon (Pritz & Ruan, 2009). In *Pseudemys scripta*, Pax6 was expressed in the telencephalon (olfactory bulb, dorsal septum, striatum, and amygdaloid complex), diencephalon (pretectum and prethalamus), mesencephalon (dorsal tegmentum), rostral medulla, ventricular zone of the entire medullary alar plate, and granule cell layer of the cerebellum (Moreno *et al*., 2014). The distribution pattern of Pax6 in the brain of *M. reevesii* observed in this study was highly consistent with these findings. This suggested that despite the morphological diversity of reptilian brains, Pax6 distribution across different brain regions remained evolutionarily conserved. The stable expression pattern of Pax6 reflected tightly constrained neurodevelopmental pathways among different reptilian species.

CONCLUSION

This study investigated the anatomical and histological structure of the *M. reevesii* brain and revealed the distribution pattern of Pax6 across various brain regions in juvenile *M. reevesii*.Pax6 showed varying expression levels in different brain areas. These findings provided a basis for future research on Pax6's role and mechanisms in *M. reevesii* brains.

LIU, R; LIU, P.; CHEN, H.; WANG, Y.; LI, Z.; LIU, Z. & NIE, L. Histología y análisis de inmunofluorescencia en el cerebro de la tortuga de Reeve (*Mauremys reevesii*). *Int. J. Morphol., 43(6)*:1973-1980, 2025.

RESUMEN: Este estudio investigó la estructura histológica del cerebro de *Mauremys reevesii* mediante tinción con hematoxilina-eosina (HE) y examinó la localización y expresión de Pax6 en el cerebro mediante tinción de inmunofluorescencia. Los resultados de la tinción con HE revelaron las estructuras histológicas en el bulbo olfatorio, el cerebro, el diencéfalo, el mesencéfalo, el cerebelo y la médula oblonga de *M. reevesii*. El bulbo olfatorio se puede dividir en siete capas, desde la región externa hasta la interna. La corteza cerebral consta de tres capas. El techo óptico del mesencéfalo comprendía seis capas distintas. La corteza cerebelosa exhibía una organización triestratificada. En *M. reevesii*, si bien el tálamo y la médula oblonga carecían de una organización laminar distintiva, contenían numerosos núcleos. La tinción de inmunofluorescencia reveló una distribución generalizada de células inmunorreactivas a Pax6 (Pax6-IR) en el cerebro de *M. reevesii*. En el bulbo olfatorio, las células Pax6-IR se distribuían densamente en la capa glomerular. Dentro del telencéfalo, estas células mostraron la mayor densidad y la mayor intensidad de fluorescencia en el tabique dorsal. En el diencéfalo de *M. reevesii*, el pretálamo contenía extensas poblaciones de células Pax6-IR. Dentro del mesencéfalo, se observó una prominente inmunorreactividad a Pax6 en el tegmento. En cortes coronales, se observaron células Pax6-IR continuas distribuidas prominentemente a lo largo de la porción dorsal de la médula oblonga, cerca de la región de la placa alar del cuarto ventrículo. En el cerebelo, se observó una inmunorreactividad extensa de Pax6 tanto en la capa medular como en la capa granular, aunque con menor intensidad de fluorescencia.

PALABRAS CLAVE: Cerebro de ***Mauremys reevesii*****; Tinción HE; Pax6; Tinción de inmunofluorescencia.**

REFERENCES

Bandín, S.; Morona, R.; López, J. M.; Moreno, N. & González, A. Immunohistochemical analysis of Pax6 and Pax7 expression in the CNS of adult *Xenopus laevis*. *J. Chem. Neuroanat., 57-58*:24-41, 2014.

Dacey, D. M. & Ulinski, P. S. Optic tectum of the eastern garter snake, *Thamnophis sirtalis*. II. Morphology of efferent cells. *J. Comp. Neurol., 245(2)*:198-237, 1986.

Daems, C.; Baz, E. S.; D'Hooge, R.; Callaerts-Vegh, Z. & Callaerts, P. Gene expression differences in the olfactory bulb associated with differential social interactions and olfactory deficits in Pax6 heterozygous mice. *Biol. Open, 14(2)*:BIO061647, 2025.

Foster, R. E. & Hall, W. C. The connections and laminar organization of the optic tectum in a reptile (*Iguana iguana*). *J. Comp. Neurol., 163(4)*:397-425, 1975.

Jiménez, S.; Santos-Álvarez, I.; Fernández-Valle, E.; Castejón, D.; Villa-Valverde, P.; Rojo-Salvador, C.; Pérez-Llorens, P.; Ruiz-Fernández, M. J.; Ariza-Pastrana, S.; Martín-Ortí, R.; González-Soriano, J. & Moreno, N. Comparative MRI analysis of the forebrain of three Sauropsida models. *Brain Struct. Funct., 229(6)*:1349-64, 2024.

Kálmán, M.; Kiss, A. & Majorossy, K. Distribution of glial fibrillary acidic protein-immunopositive structures in the brain of the red-eared freshwater turtle (*Pseudemys scripta elegans*). *Anat. Embryol. (Berl.), 189(5)*:421-34, 1994.

Kondoh, D.; Wada, A.; Endo, D.; Nakamuta, N. & Taniguchi, K. Histological and lectin histochemical studies on the main and accessory olfactory bulbs in the Japanese striped snake, *Elaphe quadrivirgata*. *J. Vet. Med. Sci., 75(5)*:567-74, 2013.

Kozmik, Z. & Kozmikova, I. Ancestral role of Pax6 in chordate brain regionalization. *Front. Cell Dev. Biol., 12*:1431337, 2024.

Liu, W. & Li, Y. Studies on the micro-structure of pituitary gland and ultrastructure of adenohypophysis in *Chinemys reevesii* (in Chinese). *Acta Hydrobiol. Sin., 29(6)*:661-6, 2005.

López, J. M.; Morona, R.; Moreno, N.; Lozano, D.; Jiménez, S. & González, A. Pax6 expression highlights regional organization in the adult brain of lungfishes, the closest living relatives of land vertebrates. *J. Comp. Neurol., 528(1)*:135-59, 2020.

Martínez-Guijarro, F. J.; Blasco-Ibáñez, J. M. & Freund, T. F. Serotoninergic innervation of nonprincipal cells in the cerebral cortex of the lizard *Podarcis hispanica*. *J. Comp. Neurol., 343(4)*:542-53, 1994.

More, S.; Mallick, S.; Shenoy, P. S. & Bose, B. Pax6 expressing neuroectodermal and ocular stem cells: its role from a developmental biology perspective. *Cell Biol. Int., 48(12)*:1802-15, 2024.

Moreno, N.; Joven, A.; Morona, R.; Bandín, S.; López, J. M. & González, A. Conserved localization of Pax6 and Pax7 transcripts in the brain of representatives of sarcopterygian vertebrates during development supports homologous brain regionalization. *Front. Neuroanat., 8*:75, 2014.

Muñoz, M.; Smeets, W. J. A. J.; López, J. M.; Moreno, N.; Morona, R.; Domínguez, L. & González, A. Immunohistochemical localization of neuropeptide FF-like in the brain of the turtle: relation to catecholaminergic structures. *Brain Res. Bull., 75(2-4)*:256-60, 2008.

Nomura, T.; Kawakami, A. & Fujisawa, H. Correlation between tectum formation and expression of two PAX family genes, PAX7 and PAX6, in avian brains. *Dev. Growth Differ., 40(5)*:485-95, 1998.

Park, S. W.; Lee, H. N.; Jeon, G. S.; Sim, K.-B.; Cho, I.-H. & Cho, S. S. The expression of transferrin binding protein in the turtle nervous system. *Arch. Histol. Cytol., 72(1)*:65-76, 2009.

Pritz, M. B. & Ruan, Y. W. PAX6 immunoreactivity in the diencephalon and mesencephalon of alligator during early development. *Brain Behav. Evol., 73(1)*:1-15, 2009.

Sarkar, S. & Atoji, Y. Distribution of vesicular glutamate transporters in the brain of the turtle (*Pseudemys scripta elegans*). *J. Comp. Neurol., 526(10)*:1690-702, 2018.

Schechter, P. B. & Ulinski, P. S. Interactions between tectal radial cells in the red-eared turtle, *Pseudemys scripta elegans*: an analysis of tectal modules. *J. Morphol., 162(1)*:17-36, 1979.

Shen, D.; Zhang, X. & Jiang, S. Electron microscopic observations on synapses in the core nucleus of ADVROF of *Emys orbicularis* (in Chinese). J. Guangxi Norm. Univ., 12(2):74-80, 1994.

Smeets, W. J. A. J.; López, J. M. & González, A. Immunohistochemical localization of DARPP-32 in the brain of the turtle, *Pseudemys scripta elegans*: further assessment of its relationship with dopaminergic systems in reptiles. *J. Chem. Neuroanat., 25(2)*:83-95, 2003.

Ueda, S.; Takeuchi, Y. & Sano, Y. Immunohistochemical demonstration of serotonin neurons in the central nervous system of the turtle (*Clemmys japonica*). *Anat. Embryol. (Berl.), 168(1)*:1-19, 1983.

Yang, C.; Li, L.; Kou, Z.; Zhang, H.; Wang, L.; Zhao, Y. & Zhu, N. Telencephalon cytoarchitecture of Tsinling dwarf skinks (*Scincella tsinlingensis*). Micron, 130:102799, 2020.

Zhang, B.; Hou, M.; Huang, J.; Liu, Y.; Yang, C. & Lin, J. Pax6 regulates neuronal migration and cell proliferation via interacting with Wnt3a during cortical development. *Sci. Rep., 15(1)*:4726-45, 2025.

Corresponding author:
Zaiqun Liu
College of Life Sciences
Anhui Normal University
No. 2 Beijing East Road
Wuhu
Anhui 24100
CHINA

E-mail: liuzaiqun@126.com